EFFECT OF CORROSION-INDUCED HYDROGEN EMBRITTLEMENT ON THE FRACTURE TOUGHNESS OF 2024-T3 ALUMINUM ALLOY

P. Papanikos
ISTRAM, Institute of Structures and Advanced Materials, 57 Patron-Athinon Road, Patras 26441, Greece

Al. Th. Kermanidis
Laboratory of Technology & Strength of Materials, Dept. of Mechanical Engineering & Aeronautics, University of Patras, 26500 Patras, Greece

Abstract

An experimental investigation is carried out to examine the effect of corrosion-induced hydrogen embrittlement on the mechanical behavior and fracture toughness of 2024-T3 aluminium alloy. The observed dramatic reduction in tensile ductility was associated with the reduction of the residual strength of corroded components. The results support early findings that corrosion of 2024-T3 aluminium alloy is associated to localized hydrogen embrittlement. A model, based on a mesodamage concept, was used to relate the reduction of fracture toughness and residual strength to the reduction of the strain energy density obtained from tensile tests on corroded and un-corroded coupons. It has been shown that the strain energy density can be used to reliably predict the residual strength of corroded components.

Keywords: Corrosion, hydrogen embrittlement, strain energy density, fracture toughness, residual strength, aluminium alloys, aging aircraft.

1. Introduction

For the evaluation of the structural integrity of ageing aircraft components the effect of corrosion has to be accounted for since corrosion and the associated hydrogen embrittlement of high strength aluminium alloys can lead to catastrophic failure. The effect of corrosion-induced hydrogen embrittlement can be attenuated when corrosion interacts with other form of damage such as a single fatigue crack or multiple site damage [1]. Numerous committees and international conferences have been organized [2-3] to ponder on the problem of material degradation in older aircraft and one important issue is corrosion [4-5]. Currently, corrosion and hydrogen damage mechanisms of aluminium alloys are far from being understood. The damage processes involved occur in atomic scale. Corrosion attack of aluminium alloys has been attributed to the complex process of oxidation [e.g. 1, 6]. Yet, it has been recognized that additionally to oxidation processes, hydrogen produced during the corrosion process may diffuse to the material interior and lead to hydrogen-metal interaction [e.g. 7]. The hydrogen trapping sides depend on the alloy system [7-14]. In [9] the determined em-

brittlement of the Al-Mg and Al-Zn-Mg aluminium alloy systems was explained as the result of the formation of magnesium hydrides on the grain boundaries. Yet, a dramatic embrittlement of the alloys 2024 following exposure in several corrosive environments has been reported in [7, 10-12]; 2024 belongs to the Al-Cu system. The same behavior was observed for the 6013, 8090 and 2091 alloys as well. In [13] hydrogen trapping sides for the Al-Cu alloy 2024 are identified.

In [15] the authors have shown that the fracture toughness of the corroded material decreases significantly and that it is necessary to evaluate a local fracture toughness associated with the reduction of strain energy density. It was shown that the proposed mesomechanics approach is very efficient for facing the complex interactive corrosion-hydrogen embrittlement process and it was suggested to examine the effect of corrosion-induced hydrogen embrittlement on MSD problems where the distance of the rivet holes is such that allows local volumetric embrittlement of the material. This work is an extension of the work in [15] to take into account the above raised issues.

In the present work the meso-damage approach introduced in [15] is used to relate the reduction of fracture toughness and residual strength to the reduction of the strain energy density obtained from tensile tests on corroded and un-corroded coupons. In addition to tensile tests, residual strength tests were conducted using notched pre-fatigued (MSD) specimens containing a row of two holes. Both corroded and un-corroded specimens were tested.

2. Mesodamage approach

Corrosion is the result of complex oxidation processes at atomic scale. Hydrogen embrittlement is a diffusion-controlled process and it is associated with the concentration and trapping of hydrogen at preferable trapping sides. The process takes place at atomic scale as well. The severity of the hydrogen damage depends on location and time. As such a process, embrittlement evolution in a thick specimen or component is linked to the concentration of hydrogen atoms. Embrittlement reaches its maximum value at the surface layer, which is saturated with trapped hydrogen and decreases gradually with decreasing concentration of hydrogen.

This process may be interpreted as the embrittlement of three-dimensional meso-volumes, which exhibit different degree of embrittlement. It yields to varying mechanical properties and fracture toughness at the meso-level. The tensile tests described underneath can be used to evaluate these varying tensile properties and fracture toughness. In diffusion controlled processes same concentration of the diffusing medium can be achieved at short distances from the source of the diffusing medium and short diffusion times or at long distances from the source and long times. Thus, the properties of specimens subjected to different exposure times can be interpreted to reflect the average properties of a number of prospective meso-volumes at different distances from the surface. Early experimental results [5, 14] indicate that hydrogen diffusion is very low from the front and back surface of the specimens and high from the edges and through the thickness cuts. Obviously the specimen thickness of 1.6mm is too large as compared to the size of meso-volumes typically not exceeding a few microns. Yet, as shown in [14] the hydrogen may diffuse at distances larger than 25mm. Thus, the properties of the meso-volumes lying along the path of hydrogen diffusion may be approximated through prospective average values derived each time for a number of meso-volumes involved in 1.6mm distance. With regard to the diffusion controlled embrittlement process the varying degree of embrittlement at different distances from the hydrogen source may be simulated through the exposure of specimens of same thickness (here 1.6mm)

for different times at same corrosive environment.

3. Experimental investigation

The experimental investigation was performed on the aluminium alloy 2024-T3 with the following chemical composition: 0.10% Si, 0.18% Fe, 4.35% Cu, 0.67% Mn, 1.36% Mg, 0.02% Cr, 0.07% Zn, 0.03% Ti, 0.01% Zr. The alloy was received in sheet form of 1.6mm nominal thickness. Tensile, fracture toughness, and MSD specimens were prepared. Tensile specimens were machined according to ASTM E8m-94a; specimens were cut in both longitudinal (L) and long transverse (LT) direction. Fracture toughness specimens were cut in (L) direction following the ASTM E561-94 specification.

The tensile and fracture toughness specimens were exposed to an exfoliation corrosion environment according to specification ASTM G34-90. The corrosive solution consists of chemicals diluted in 1 l distilled water. They are sodium chloride (4.0 M NaCl, potassium nitrate (0.5 M KNO_3) and nitric acid (0.1 M HNO_3). The initial apparent pH of the solution was 0.4. The solution volume per exposure area was 17.5 ml/cm^2 and the solution temperature was 17.5 ± 3^oC. The specimens were exposed to the solution for a number of different exposure times. After exposure, specimen cleaning was conducted according to ASTM G34-90. Then the corroded specimens were subjected to mechanical testing.

The MSD specimens (Fig. 1) were flat specimens containing a row of two holes in order to examine the effect of corrosion on the residual strength. Two notches were machined on both sides of the holes and the specimens were pre-fatigued to a certain crack length. The MSD specimens were embedded in the exfoliation corrosion solution while different loads were applied and the time to failure was recorded.

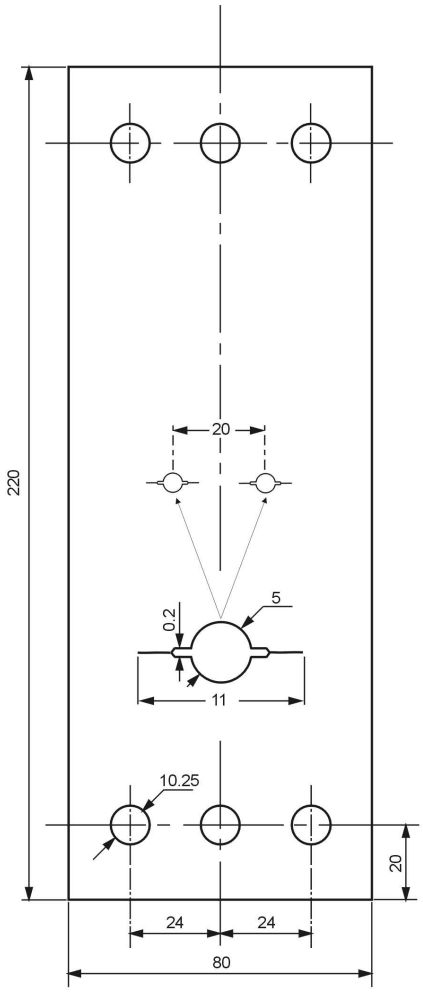

Figure 1: *Schematic of the MSD specimen.*

4. Results and discussion

Mechanical characterization.

The tensile properties of the reference material are summarized in Table 1. The energy density is evaluated by the area under the true stress-strain curve.

The residual mechanical properties as a percentage of the properties of the reference material are shown in Fig. 2 for the L directions of (a) bare specimens and (b) Al-clad specimens. For the case of bare specimens, the figure shows the property decrease trend versus exposure time in exfoliation corrosion solution. All properties decreased non-linearly with exposure time. It is clear from Fig. 2(a) that yield and ultimate tensile stress have been practically not affected. On the contrary, a

Material	Yield stress, S_y [MPa]		Ultimate tensile stress, R_m [MPa]		Elongation to failure, A_{50} [%]		Energy density, W [MJ/m^3]	
	L	LT	L	LT	L	LT	L	LT
2024-T3	396	339	520	488	18.0	18.0	86.7	81.7

Table 1: *Tensile properties for reference material.*

clear trend of an appreciable tensile ductility decrease has been observed. Obtained yield and ultimate tensile stress decrease is caused by corrosion induced material surface degradation.

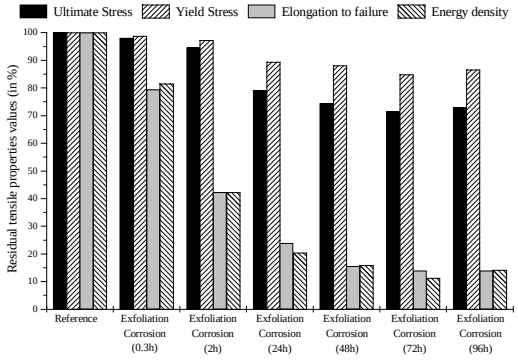

(a)

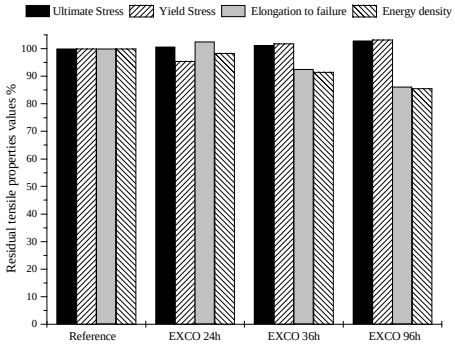

(b)

Figure 2: *Gradual tensile property degradation for the alloy 2024 (L-direction) during exposure in exfoliation corrosion solution: (a) bare, (b) Al-clad.*

It was found that after machining of the corrosion attacked material surface layer, yield and ultimate tensile stress increase again almost to their initial values. Yet, tensile ductility drop is volumetric. Machining of the corrosion attacked surface layer had practically no influence on the determined tensile ductility values although the tensile tests were performed on the "non-corroded" material core after the removal of the corrosion-attacked layer. In [13], the observed bulk embrittlement has been associated to hydrogen penetration and absorption. Similar trends show the tensile properties in the LT direction. For the Al-clad specimens, the results of Fig. 2(b) reveal that the tensile properties are only slightly affected by the corrosion exposure. It is believed that the reason for this is that cladding acts as a cathodic corrosion protection.

Fracture Toughness.

Fig. 3 shows the fracture surfaces of a non-corroded (a) and a corroded fracture toughness specimen (b). It is clear from the figures that the mode of final failure is different for the two cases. In the non-corroded specimen, a typical ductile fracture is observed. However, a brittle fracture is observed in the corroded specimen indicating that the corrosion-induced embrittlement goes far beyond the corroded layer of the material, which for the specimen showing in Fig. 3(b) has a depth of 200 mm. The failure surface indicates the gradual change from a brittle to a ductility failure with increasing distance from the corroded area. Table 2 shows the fracture toughness tests conducted and the values of fracture toughness obtained. For the case of protected specimens (anodizing and sealing), no corrosion effect was observed. The small decrease of the fracture toughness as compared to the un-protected

reference specimens might be attributed to the fact that the process of anodization leads to material embrittlement. The results for the un-protected specimens indicate that corrosion leads to a significant decrease in fracture toughness (27%). Yet, the dimensions of the specimen are by far larger as the distance within hydrogen may diffuse. The values of the fracture toughness obtained reflect specimens, which are partially fully embrittled, in certain locations only partially embrittled to different degrees of embrittlement and, far from the hydrogen source, not embrittled at all. The approach described underneath will be utilized to yield to local fracture toughness values. Following to the work in [16], the strain energy density evaluated from the stress-strain curve of the material can be associated to the fracture toughness with the relation:

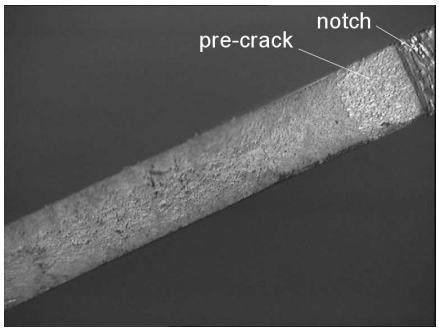

(a)

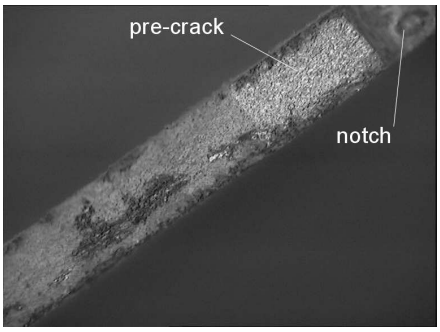

(b)

Figure 3: *Fracture surfaces of a (a) non-corroded and (b) corroded (EXCO 36 h) fracture toughness specimens.*

$$K_c^2 \propto \Phi W_0 \quad (1)$$

where K_c is the fracture toughness, W_0 the strain energy density and Φ a function of the elastic properties of the material. The quantity Φ will be considered constant with corrosion exposure. Eq. 1 can be used to estimate the value of K_c for an embrittled material due to corrosion since it suggests that

$$K_{ct}^2 / K_c^2 \approx W_t / W_0 \quad (2)$$

where K_{ct} and W_t are the fracture toughness and the strain energy density, respectively, after t hours of exposure to corrosion. Using the values of Table 1 and the results of Fig. 2(a), it can be estimated that the value of energy density for 36 h exfoliation corrosion is $W_{36} \approx 14.7\ MJ/m^3$. From Tables 1 and 2 we have that $K_c \approx 134.6\ MPa\sqrt{m}$ and $W_0 \approx 86.7\ MJ/m^3$. Therefore, Eq. 2 gives $K_{c36} \approx 55.4\ MPa\sqrt{m}$. This value is however much smaller than the measured value of $97.8\ MPa\sqrt{m}$. The reason for this discrepancy is that the fracture toughness specimen does not experience volumetric embrittlement as the tensile specimen used to obtain the strain energy density. The above observation is very important as far as the structural integrity of a corroded aircraft structure is concerned. It indicates that the use of the virgin material fracture toughness for assessing the structural integrity of aged and corroded components may result to essential overestimation of residual strength, which could lead to fatal consequences. On the other hand, the use of the value of fracture toughness evaluated assuming volumetric embrittlement of the material can be very conservative and lead to over sizing. It is therefore necessary for a specific problem to use a local fracture toughness, which will range from the minimum value (volumetric embrittlement) to the maximum value of the vir-

Material 2024-T3	Corrosion exposure	Direction/ number of tests	K_c [$MPa\sqrt{m}$]
Reference, t=1.6mm	None	L/2	134.6
Corroded, t=1.6mm	EXCO 36 h	L/2	97.8
Reference (anodized and sealed), t=1.6 mm	None	L/2	126.5
Corroded (anodized and sealed), t=1.6mm	EXCO 36 h	L/2	125.2

Table 2: *Fracture toughness test results.*

gin material. This is especially true for MSD problems where the distance of the rivet holes is such that allows local volumetric embrittlement of the material.

Residual strength.

To overcome the difficulties mentioned above and evaluate the residual strength of simple "MSD" problems, the tests described in section 3 were performed. It is clear, however, that the specimen shown in Fig. 1 cannot produce values of K_c, since the size of the cracks involved is very small. Yet, it was selected in order to achieve volumetric embrittlement between the two adjacent holes, since the distance between them is of the same order as the width of the tensile specimens. Furthermore, the distance between the two holes is a realistic representation of rivet distances in aircraft structural components, which may suffer from MSD. The type of failure in the MSD specimens would be expected to be a combination of fracture and net-section yielding. However, it is believed that the reduction in residual strength of the components with corrosion exposure would be directly related to the reduction of the strain energy density as measured from the tensile tests. It should be noted here that no significant crack growth was observed prior to failure, except for the last test (336h). This is in agreement with [17] where it is stated that exfoliation corrosion does not lead to significant stress corrosion cracking.

Table 3 shows the results of the residual strength measurements. If we denote by R_t the strength of the coupon after t hours of exposure to corrosion, then it is safe to assume, similar to Eq. 1 that:

$$R_t^2 / R_0^2 \square W_t / W_0 \qquad (3)$$

Using Eq. 3, the values of W_t / W_0 are evaluated in Table 3.

Corrosion exposure	Strength [kN]	W_t / W_0 [%]
None	27.13	100
EXCO 10 h	14.72	29.4
EXCO 72 h	11.50	18.0
EXCO 336 h	8.96	10.9

Table 3: *Residual strength test results.*

Fig. 4 shows the percentage reduction in the strain energy density from the tensile tests and the MSD tests. It is clear that both results fit well. This suggests that we can use the results of the tensile tests to evaluate the strength of corroded components if we know the strength of the uncorroded component. Further experimental investigation is currently conducted in order to support this evidence with other

aluminium alloys, thickness and coupon configurations.

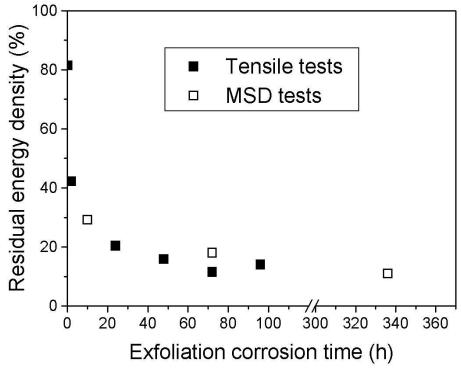

Figure 4: *Residual energy density from tensile and MSD tests.*

5. Conclusions

An experimental investigation was carried out to examine the effect of corrosion-induced hydrogen embrittlement on the tensile behavior and fracture toughness of 2024-T3 aluminium alloy. A mesodamage approach and the strain energy density theory were used to relate tensile properties with the residual strength of simple components. The work indicates the following:

- Corrosion-induced degradation of mechanical properties occurs gradually with the exposure time. Tensile ductility decreases exponentially to extremely low final values.
- The fracture toughness of the corroded material decreases significantly. It is necessary to evaluate a local fracture toughness associated with the reduction of strain energy density.
- The use of the strain energy density reduction as measured from tensile tests can be used to evaluate the reduction of residual strength of structural components due to corrosion-induced hydrogen embrittlement.

References

[1] Inman, M.E., Kelly, R.G., Willard, S.A. and Piascik R.S. (1997) In: Proceedings of the FAA-NASA Symposium on the Continued Airworthiness of Aircraft Structures, pp. 129-146, Springfiled, Virginia.

[2] FAA-NASA Symposium on the Continued Airworthiness of Aircraft Structures, FAA Center of Excellence in Computational Modeling of Aircraft Structures, Atlanta, USA, 1996.

[3] AGARD Workshop, *Fatigue in the Presence of Corrosion*, RTO Meeting Proceedings 18, Corfu, Greece, 1999.

[4] BRITE/EURAM 1053, Structural Maintenance of Aging Aircraft (SMAAC), CEC Brussels, Final Report, 1999.

[5] EPETII/30 (1999). *Damage Tolerance Behavior of Corroded Aluminum Structures.* Final Report, General Secretariat for Research and Technology, Greece.

[6] Smiyan, O.D., Koval, M.V. and Melehkov, R.K., (1983*), Soviet Mater. Sci*., **19**, pp. 422.

[7] Pantelakis, Sp.G., Vassilas, N.I. and Daglaras, P.G., (1993), *Metall*, **47**, pp. 135.

[8] Scaman, G.M., Alani, R. and Swann, P.R., (1976), *Corrosion Science*, **16**, pp. 443.

[9] Tuck, C.D.S. (1980) In: Proceedings of the 3rd Int. Conference of Hydrogen on the Behavior of Materials, pp. 503-510, Jackson, USA.

[10] BRITE/EURAM BE92-3250, Investigation on Aluminium-Lithium Alloys for Damage Tolerance Applications, Final Report, CEC Brussels, 1993.

[11] Pantelakis, Sp.G., Kermanidis, Th.B., Daglaras, P.G. and Apostolopoulos, Ch.Alk. (1998) In: Fatigue in the Presence of Corrosion, AGARD Workshop, Corfu, Greece.

[12] Pantelakis, Sp.G., Daglaras, P.G. and Apostolopoulos, Ch.Alk. (2000), *J. Theor. Appl. Fract. Mech*., **33**, pp. 117.

[13] Haidemenopoulos, G.N., Hassiotis, N., Papapolymerou G. and Bontozoglou V., (1998), *Corrosion*, **54**, pp. 73.

[14] PENED99/649 (2001). *Corrosion and Hydrogen Embrittlement of Aircraft Aluminum Alloys.* Final Report, General Secretariat for Research and Technology, Greece.

[15] Kermanidis, Al.Th., Papanikos, P., and Pantelakis, Sp.G. (2001) In: CD-ROM Proceedings of ICF10: Advances in Fracture Research, Ravi-Chandar, K., Karihaloo, B.L., Kishi, T., Ritchie, R.O., Yokobori Jr. and Yokobori, T. (Eds). Elsevier Science Ltd., UK.

[16] Jeong, D.Y., Orringen, O. and Sih, G.C. (1995), *J. Theor. Appl. Fract. Mech*., **22**, pp. 127.

[17] Aluminum and Aluminum Alloys, ASM Specialty Handbook, Davis, J.R. (Ed.), Davis & Associates, ASM International, 1993.